

## Some Implications of Combined X-ray and Neutron Diffraction Studies\*

BY PHILIP COPPENS

Chemistry Department, State University of New York at Buffalo, Buffalo, New York 14214, U.S.A.

(Received by the Hamilton Symposium Committee 17 July 1973)

A survey is made of about ten combined X-ray and neutron diffraction studies. The theory of X-N difference densities is reviewed for both centric and acentric structures. It is concluded that the phase problem has been incorrectly treated in past work on *acentric* crystals, leading to a systematic underestimate of the difference density. Expressions are given for the average standard deviation in the difference density due to random errors in both the X-ray and neutron measurements. A survey of experimental peak heights indicates that (a) the peaks in lone-pair regions are generally lower than the maxima in the bonds, (b) double bonds may have lower difference densities than either triple or single bonds. The effect of thermal smearing on a theoretical difference density is analyzed and it is shown that the relatively low height of the lone-pair density is a result of molecular vibrations which affect the sharper lone-pair features more strongly than the overlap density. The first-row atom asphericity shifts are reviewed and discussed in terms of scattering factors associated with the difference density features. The size of the shifts varies with data cut-off and thermal amplitude of the atoms, as the lone pair scattering is relatively dominant in the high-order region.

### Introduction

'Do you feel that you are now using the theory to calibrate the experiment but as you go along to larger and larger molecules the experiment will play the dominant role in getting out the really chemically interesting information?' Walter C. Hamilton ACA Symposium, Albuquerque (1973).

It seems appropriate at this time to discuss how well the experiment has been calibrated by theoretical calculations and to examine information available from very few studies on larger molecules.

### Survey of structures studied

The number of compounds that have been studied by the combined X-ray-neutron technique is limited, because the studies are time-consuming and require careful attention to details of both the X-ray and neutron experiments. A listing of published studies is given in Table 1. They fall in three groups: room-temperature studies of centric (1) and acentric (3) crystals and liquid nitrogen temperature studies of centric crystals (2). The resulting X-ray neutron difference density  $\rho_{X-N}$ , which is further defined below represents the redistribution of the electron density when atoms bond to form a molecule. An example is given in Fig. 1, which shows  $\rho_{X-N}$  in the plane of the tetracyanoethylene molecule (Becker, Coppens & Ross, 1974). Typically, density is accumulated in the bonds between the atoms and in the lone pair at the 'free' side of the

nitrogen atom. The nitrogen atom and the ethylenic carbon atom are in negative regions indicating an outflow of electrons into the bonds and lone pairs. The cyano carbon atom is less typical, the density at its nucleus being positive. The physical significance of this finding is doubtful as errors in  $\rho_{X-N}$  accumulate at atomic positions (see below). Further examples of the confirmation of theoretical concepts are found in the studies on decaborane (Brill, Dietrich & Dierks, 1971) and tetracyanoethylene oxide (TCEO) (Matthews & Stucky, 1971). In decaborane density is found *within* the BHB triangles (Fig. 2) rather than in the bonds as expected for a three-center bond. In TCEO (Fig. 3) an appreciable accumulation of density is found *outside* the COC triangles, thus supporting the concept of bond-bending in strained ring systems (Coulson & Moffitt, 1949).

Table 1. Survey of comparative X-ray and neutron studies (June 1973)

(1) Centrosymmetric, room-temperature		
<i>s</i> -Triazine		Coppens (1967)
Oxalic acid.H <sub>2</sub> O		Coppens, Sabine, Delaplane & Ibers (1969)
Tetracyanoethylene oxide		Matthews & Stucky (1971)
Tetracyanoethylene		Becker, Coppens & Ross (1974)
(2) Centrosymmetric, liquid N <sub>2</sub>		
Cyanuric acid		Coppens & Vos (1971)
Decaborane		Brill, Dietrich & Dierks (1971)
Benzenechromium tricarbonyl		Rees & Coppens (1973)
(3) Acentric, room-temperature		
Sucrose		Hanson, Sieker & Jensen (1973)
Ammonium oxalate H <sub>2</sub> O		Taylor & Sabine (1972)
Hexamethylenetetramine		Duckworth, Willis & Pawley (1970)

\* *Editorial note*:— This paper was presented at a memorial symposium in honour of Walter C. Hamilton, a former Co-editor of *Acta Crystallographica*, held on 15 June 1973 at Brookhaven National Laboratory, and sponsored jointly by the American Crystallographic Association and the Brookhaven National Laboratory.

How well do the experimental densities agree quantitatively with predictions from theoretical calculations? Before attempting to answer this question we will first review the theory of X-N maps and analyze the effect of experimental errors on the difference density.

### Theory of X-N difference densities

The difference density  $\rho_{X-N}$  at the point  $\mathbf{r}$  in the unit cell is defined as:

$$\rho_{X-N}(\mathbf{r}) = \frac{1}{V} \sum_{\text{all observations}} (\mathbf{F}_{\text{obs}, X} - \mathbf{F}_{\text{calc}, N}) \exp(-2\pi i \mathbf{H} \cdot \mathbf{r}) \quad (1)$$

where  $\mathbf{H} = (hkl)$ ,  $\mathbf{F}_{\text{obs}, X}$  is the observed X-ray structure amplitude with appropriate phase and  $\mathbf{F}_{\text{calc}, N}$  is the structure factor calculated with isolated-atom X-ray form factors  $f_{i, X}$  but neutron positional parameters ( $r_{i, N}$ ) and neutron temperature factors ( $T_{i, N}$ ):

$$\mathbf{F}_{\text{calc}, N} = \sum_{\text{atoms}} f_{i, X} \exp(2\pi i \mathbf{H} \cdot \mathbf{r}_{i, N}) T_{i, N}$$

### Systematic errors in acentric summations

In the centrosymmetric case (1) reduces to

$$\rho_{X-N}(\mathbf{r}) = \frac{1}{V} \sum_{\text{all observations}} \left( F_{\text{obs}, X} \frac{|F_{\text{calc}, X}|}{F_{\text{calc}, X}} - F_{\text{calc}, N} \right) \times \cos 2\pi \mathbf{H} \cdot \mathbf{r} \quad (2)$$

The sign factor  $|F_{\text{calc}, X}|/F_{\text{calc}, X}$  may be replaced with confidence by  $|F_{\text{calc}, N}|/F_{\text{calc}, N}$  as the deviations from spherical symmetry are sufficiently small to make sign changes rare exceptions.

In the acentric structure, however, use of the phase  $\varphi_{\text{calc}, N}$  introduces considerable systematic errors, because it corresponds to the summation

$$\rho_{X-N}(\mathbf{r}) = \frac{1}{V} \sum_{\text{all observations}} (|F_X| - |F_N|) \exp i\varphi_N \exp(-2\pi i \mathbf{H} \cdot \mathbf{r})$$

in which the amplitude  $|F_X| - |F_N|$  is always smaller than the correct choice of  $|F_X - F_N|$  and the phase  $\varphi_N$  (or  $\varphi_N + \pi$  if  $|F_X| < |F_N|$ ) is appreciably different from the phase that corresponds to  $F_X - F_N$  (Fig. 4).

In sucrose (Hanson, Sieker & Jensen, 1973) the mean difference between the phases from the conventional X-ray refinement and from the calculation of  $F_N$  is reported to be  $1.8^\circ$ . This is likely to be an underestimate of  $\varphi_X - \varphi_N$ , because the conventional refinement does account for only part of the bond density through an adjustment of the least-squares parameters. But it agrees qualitatively with a model calculation (Coppens, unpublished) which leads to a r.m.s. phase dis-

crepancy of about  $3^\circ$  for data with  $0 < \sin \theta/\lambda < 0.5 \text{ \AA}^{-1}$ . Unfortunately, the effect of this small phase error on the amplitude and phase of the difference vector can be quite pronounced. The numerical example given in Fig. 5 shows that typical errors of 50% in the ampli-

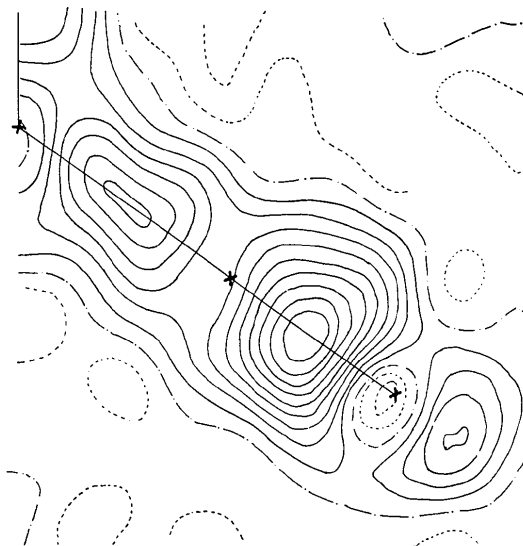


Fig. 1. Section of the function  $\Delta\rho_{X-N}$  through the molecular plane of tetracyanoethylene. Contours at  $0.10 \text{ e \AA}^{-3}$ . Negative contours ---. Zero contour - - - The cross to the right indicates the position of the nitrogen atom. The carbon atoms are to the left (Becker, Coppens & Ross, 1974).

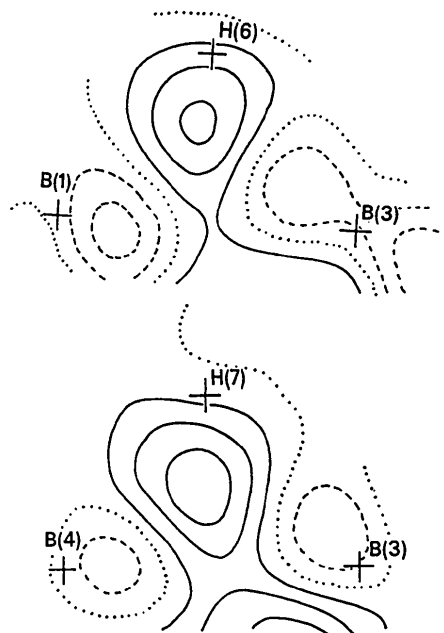


Fig. 2. Two sections of the difference density function containing BHB triangles in decaborane. Contour intervals at  $0.1 \text{ e \AA}^{-3}$  (Brill, Dietrich & Dierks, 1971).

tudes (always too small) and 45° in the phase angles may be expected. Since the acentric structures listed in Table 1 have all been analyzed using  $\varphi_N$ , the resulting

functions  $\varrho_{X-N}$  systematically underestimate the true difference density. In a better approximation  $\varphi_X$  is taken as obtained from the X-ray refinement and  $\varphi_{X-N}$ , the phase of the vector  $F_X - F_N$  is calculated as implied by Fig. 4. A further improvement should be achievable by determining  $\varphi_X$  in a refinement with a more flexible model capable of producing essentially featureless difference maps.

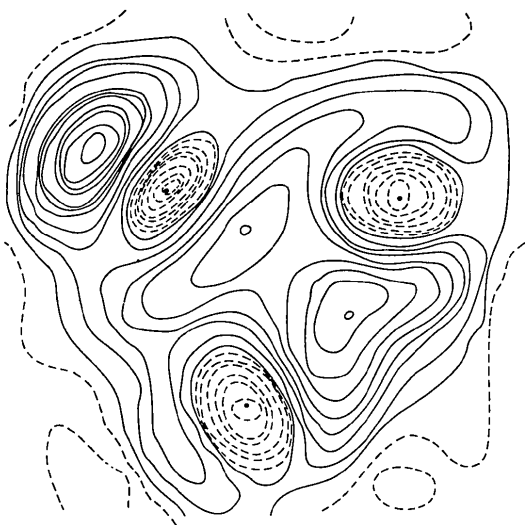


Fig. 3. Section of the difference density function through the COC triangle in tetracyanoethylene. Contours at  $0.05 e \text{ \AA}^{-3}$ . Negative and zero contours broken (Matthews & Stucky, 1971).

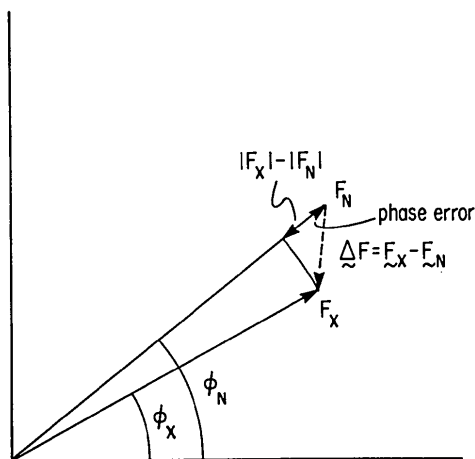


Fig. 4. Phase angles in the acentric case.

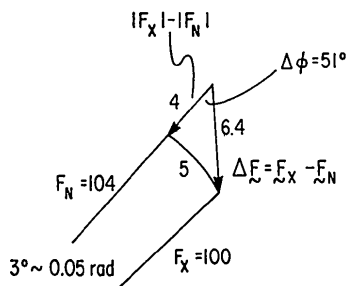


Fig. 5. Phase angles in the acentric case, numerical example with  $\Delta\varphi = 3^\circ$  and  $|F_N| - |F_X| = 0.04 |F_X|$ .

**Random errors in  $\varrho_{X-N}$**

From

$$\varrho_{X-N}(\mathbf{r}) = \frac{2}{V} \sum_0^\infty |\Delta F| \cos(2\pi\mathbf{H} \cdot \mathbf{r} - \varphi_{X-N})$$

one obtains

$$\sigma[\varrho_{X-N}(\mathbf{r})] = \frac{2}{V} \sum_0^\infty [\sigma|\Delta F| \cos \alpha + |\Delta F| \sin \alpha \sigma(\varphi_{X-N})] \quad (\text{Cruickshank, 1949}) \quad (2)$$

with  $\alpha = 2\pi\mathbf{H} \cdot \mathbf{r} - \varphi_{X-N}$ , and assuming series termination errors to be negligible.

The assumption that  $\sigma|\Delta F|$  and  $\sigma(\varphi_{X-N})$  are not correlated implies that the sample distribution of the end-points of  $F_{X-N}$  is circularly symmetric and leads to:

$$\sigma^2(\varrho_{X-N}) = \frac{4}{V^2} \sum_0^\infty [\sigma^2|\Delta F| \cos^2 \alpha + |\Delta F|^2 \sigma^2(\varphi_{X-N}) \sin^2 \alpha] \quad (3)$$

$\sigma(\varrho_{X-N})$  varies through the unit cell. The error averaged over the unit cell is given by

$$\langle \sigma^2(\varrho_{X-N}) \rangle = \frac{2}{V^2} \sum_0^\infty [\sigma^2|\Delta F| + |\Delta F|^2 \sigma^2(\varphi_{X-N})] \quad (4)$$

The second term appears only for the acentric case and can give a considerable contribution because of the ambiguity in obtaining  $\varphi_X$  (see above).

Model calculation on some simple structures show that in the centrosymmetric case (4) is a useful approximation to (3) (Coppens & Hamilton, 1968).

The error in  $|\Delta F|$  in (4) can result from errors in both the X-ray and neutron measurements. Some of these errors in an X-ray and a neutron measurement may be correlated. For example, the effect of thermal diffuse scattering (TDS) in X-ray and neutron measurements is similar, apart from differences in the instrumental resolution functions (Willis, 1969). Such errors will tend to cancel when the function  $\varrho_{X-N}$  is calculated.

To the extent that  $\sigma(F_X)$  and  $\sigma(F_N)$  are not correlated, one gets for the centric case:

$$\begin{aligned} \langle \sigma^2(\varrho_{X-N}) \rangle &= \frac{2}{V^2} \sum_0^\infty \sigma^2|\Delta F| \\ &= \frac{2}{V^2} \left[ \sum_0^\infty \sigma^2(F_X) + \sum_0^\infty \sigma^2(F_N) \right] \quad (5) \end{aligned}$$

The first term represents the errors in the X-ray observations and includes errors in the scale factor  $k$ : if

$$F_X = \frac{F'_X}{k}$$

$$\sigma(F_X) = \frac{\sigma(F'_X)}{k} + \frac{F'_X}{k^2} \sigma(k) = \frac{\sigma(F'_X)}{k} + F_X \frac{\sigma(k)}{k}$$

or

$$\frac{2}{V^2} \sum_0^\infty \sigma^2(F_X) = \frac{2}{V^2} \sum \frac{\sigma^2(F'_X)}{k^2} + \sum F_X^2 \frac{\sigma^2(k)}{k^2}. \quad (6)$$

The second term in (5) occurs as a result of the uncertainties in the neutron parameters  $r_{i,N}$  and  $T_{i,N}$  and is related to the error in the neutron observations  $F_{\text{neutron}}$  (different from the  $F_N$  which are calculated with X-ray scattering factors).

In first approximation

$$\sigma^2(F_N) = \left( \frac{\langle f_i \rangle}{\langle b_i \rangle} \right)^2 \sigma^2(F_{\text{neutron}})$$

where  $b_i$  is the atomic scattering length for thermal neutrons. For first row atoms  $\langle f_i \rangle \sim \langle b_i \rangle$ , so

$$\langle \sigma^2(\rho_{X-N}) \rangle \sim \frac{2}{V^2} \sum_0^\infty \{ \sigma^2(F_X) + \sigma^2(F_{\text{neutron}}) \}. \quad (7)$$

This expression for the averaged error should be used with the reservation that errors in the scale factor  $k$  (6) have the largest effect where  $\rho_X$  is large, *i.e.* at the atomic positions (Coppens, 1972). Furthermore, a bias in the neutron thermal parameters also affects the nuclear regions more than remote parts of the difference density (Stewart, 1968). Therefore, (7) should not be used as a measure of reliability near the equilibrium positions of the nuclei.

An example of the application of (7) is the study on tetracyanoethylene (TCNE) (Becker, Coppens & Ross, 1974) for which  $\sigma(\langle \rho_{X-N} \rangle)$  was estimated to be  $0.07 \text{ e } \text{\AA}^{-3}$ . Comparison with the background variation in regions away from the nuclei indicated the estimate to be reasonably pessimistic.

Finally, it is worthwhile to note that the accumulation of errors at special positions (Cruickshank & Rollett, 1953) can be avoided by collection of at least a hemisphere of diffraction data.

### Peak heights and comparison with theory

Comparison of the difference maps of the compounds listed in Table 1 confirms the reproducibility of the general appearance of the function  $\rho_{X-N}$ . How consistent are the features in similar molecular fragments in a quantitative sense?

The standard deviations in the peak heights in Table 2 are generally unknown, the only available estimate being for TCNE in which  $\sigma(\langle \rho \rangle) \sim 0.07 \text{ e } \text{\AA}^{-3}$ . We may therefore make a plea for a critical evaluation of the standard deviations in future studies of this kind. Without the benefit of standard deviations we can search for general trends in the table. Excluding the acentric structures for reasons discussed above, it appears that: (1) In several molecules C=O and C=C bonds contain lower density features than C-O and C-C single bonds. The bonding peak may be reduced because the spherical atoms subtracted to obtain the maps are at shorter distance in the shorter bonds. This effect will be opposed by the increase in bond population with bond strength which accounts for the peak heights in both TCEO and TCNE being larger in C≡N than in C-C. (2) With the exception of the oxygen lone-pair density in the strained ring of TCEO, lone-pair peaks are lower than peaks in the covalent bonds.

The latter observation contrasts sharply with the Hartree-Fock theoretical difference density map in

Table 2. Peak heights in the function  $\rho_{X-N} (\text{e } \text{\AA}^{-3})^*$

	C-C	C=C	C...N	C≡N	COH COC	C=O	CH BH	NH	OH	O, 1p	N, 1p
Group 1											
s-Triazine			0.25								0.1
Oxalic acid	0.25				0.2	0.15			0.05	0.15	
Tetracyanoethylene oxide	0.4			0.6	0.25					0.55	0.3
Tetracyanoethylene	0.6	0.4		0.9							0.4
Group 2											
Cyanuric acid			0.5			0.4		0.5		0.4	
Decaborane							0.4				
Benzenechromium tricarboxyl	0.35					0.6	0.35			0.45	
Group 3											
Sucrose	0.25				0.10	0.15	0.2		0.1	0.2	
Ammonium oxalate	0.25					0.15		0.15	0.05	0.15	

\* The numbers given correspond to the highest contour in the published density maps, or its average over equivalent bonds if differences exist.

NCCN (Fig. 6, Hirshfeld, 1971) in which the lone-pair peak height is about  $1.1 \text{ e } \text{Å}^{-3}$ , while the C–C and C≡N bond peaks reach to  $0.6$  and  $1.0 \text{ e } \text{Å}^{-3}$  respectively. Obviously, the theoretical calculations do not account for molecular vibrations which modify the experimental difference density. It is this effect that should be considered in accounting for the differences in Table 2.

We shall introduce the vibrational modification in the NCCN difference density as follows: The peak shapes in directions perpendicular to the molecular axis approximately follow a Gaussian profile. By adjusting the Gaussian at the peak and at the half-height position and ignoring the distortions from simple behavior along the molecular axis one obtains the analytical functions listed in Table 3.

Table 3. Analytical approximation to peaks in NCCN difference density ( $\text{e } \text{Å}^{-3}$ )

	Expression	Total number of electrons
C–N	$1.0 \exp(-4.56r^2)$	0.57
C–C	$0.6 \exp(-6.36r^2)$	0.21
Lone pair	$1.1 \exp(-15.11r^2)$	0.10

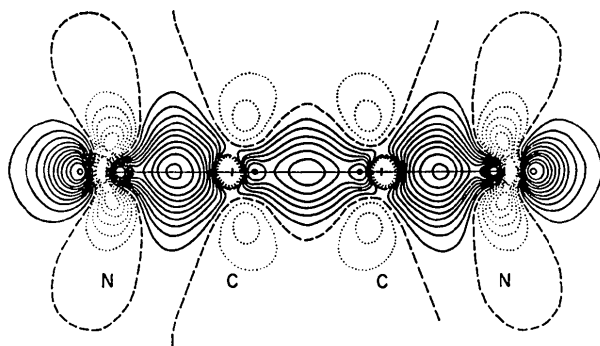


Fig. 6. Theoretical difference density in NCCN (Hirshfeld, 1971). Contour interval  $0.1 \text{ e } \text{Å}^{-3}$ . Negative contours dotted.

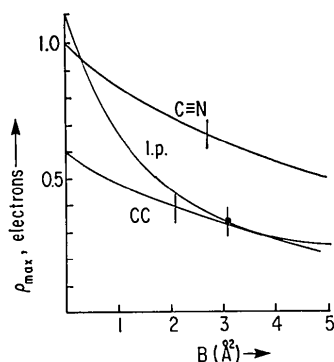


Fig. 7. Difference density peak heights in NCCN as a function of the temperature parameter  $B$  according to the single Gaussian approximation described in the text. Vertical bars indicate experimental thermal parameters.

For

$$\rho = A \exp(-\alpha r^2) \quad (8)$$

one has

$$f(\rho) = A \left(\frac{\pi}{\alpha}\right)^{3/2} \exp\left(-\frac{S^2}{4\alpha}\right), \text{ with } S = 4\pi \sin \theta/\lambda. \quad (9)$$

Introducing the vibrational modification by multiplying  $f$  by the well known Fourier transform of an isotropic harmonic smearing function (Higgs, 1953)

$$f(\langle\rho\rangle) = A \left(\frac{\pi}{\alpha}\right)^{3/2} \exp\left[-\left(\frac{S^2}{4\alpha} + \frac{BS^2}{16\pi^2}\right)\right]$$

where  $\langle\rho\rangle$  is the time-averaged density, and applying the inverse Fourier transform one obtains:

$$\langle\rho\rangle = A \frac{1}{\left(1 + \frac{\alpha B}{4\pi^2}\right)^{3/2}} \exp\left[-\frac{\alpha r^2}{\left(1 + \frac{\alpha B}{4\pi^2}\right)}\right] \quad (10)$$

which reverts to (8) for  $B=0$ .

The peak heights according to (10) are plotted in Fig. 7. The much steeper slope of the lone-pair curve is due to the sharpness of this feature in the theoretical difference density and accounts for the second experimental observation. When the appropriate values of  $B$  for TCNE are taken, the relative heights in the experimental maps are correctly predicted (Table 4). But the experimental values tend to be too large in all cases, indicating a possible scale factor error in the TCNE maps.

Table 4. Peak heights C≡N, C–C and nitrogen lone pair ( $\text{e } \text{Å}^{-3}$ )

	C≡N	C–C	Lone pair
Theoretical at rest	1.0	0.6	1.1
Theoretical at $B_{\text{experimental}}$	0.65	0.4	0.35
Experimental	0.9	0.6	0.4

\* Average of the diagonal elements of the vibrational tensors of the atoms forming the bond.

The example confirms the pronounced effect of molecular vibrations on peak heights. Calculation of temperature-corrected experimental peak heights using (10) is to be recommended for a comparison of results of different studies. It may be noted that much poorer agreement was obtained in earlier comparisons of thermally averaged theoretical difference densities from INDO (intermediate neglect of differential overlap) and minimal-basis set *ab initio* (STO-3G) calculations, with experimental data on cyanuric acid (Jones, Pautler & Coppens, 1972).

We conclude that the experiment is sensitive in the sense that it successfully discriminates against approximate theoretical calculations.

### Asphericity shifts, discrepancies between X-ray and neutron positional parameters

It is well known that the relatively large distortion of the hydrogen charge density causes a shift of the apparent X-ray hydrogen position toward the atom to which it is bonded. Hanson *et al.* (1973) found the average shift in sucrose to be 0.13 (1) Å for C–H and 0.18 (2) Å for the O–H bond. A similar but smaller effect exists for first row atoms in a pronounced asymmetric bonding environment (Coppens, Sabine, Delaplane & Ibers, 1969).

A sample of observed shifts from a comparison of X-ray and neutron data is given in Table 5. The shifts are generally in the direction of the lone-pair axes or (in the case of the cyanocarbon in TCNE) towards the density feature in the triple bond. For the nitrogen atom of the cyano group a much better balance is obtained between the triple bond and lone-pair densities and no shift is observed. This explanation is confirmed by calculations by Matthews & Stucky (1971), using a formalism for the centroid of the atomic charge density according to a simple hybridization scheme (Coppens & Coulson, 1967). This calculation ignores the effect of series termination and thermal modification and can therefore only provide a qualitative estimate. This is illustrated by the scattering factors for the NCCN difference density peaks (as approximated in Table 3), which are plotted in Fig. 8. The lone-pair scattering persists into the high order region ( $\sin \theta/\lambda > 0.6 \text{ \AA}^{-1}$ ) while the bond scattering falls off more rapidly. A possible asphericity shift of the nitrogen atom towards the lone-pair would therefore be predicted when many high-order data are included in the refinement. Such a dependence on the composition of the data set was observed in cyanuric acid (Coppens & Vos, 1971), for which the oxygen shifts average to 0.005 (1) Å for the full data refinement, but are reduced to 0.0025 Å when only data with  $\sin \theta/\lambda < 0.5 \text{ \AA}^{-1}$  are used.

As the asphericity shifts are often larger than least-squares standard deviations they affect the accuracy of X-ray crystal structure determinations. A proper correction requires a refinement with a model allowing for non-sphericity. A double-atom refinement of the X-ray data in which the valence-shell is allowed to float independently of the core-centroid does reproduce the neutron position in the case of oxalic acid dihydrate (Coppens, 1971). But the method as used assumes a spherically symmetric valence shell and therefore does not allow for valence scattering in the high order region evidenced by Fig. 8. Modification of the double-atom refinement to allow for an asymmetric valence shell is needed for more complete elimination of the asphericity shift from diffraction results.

### Conclusion

The available information indicates that the experimental measurement is comparable with the more

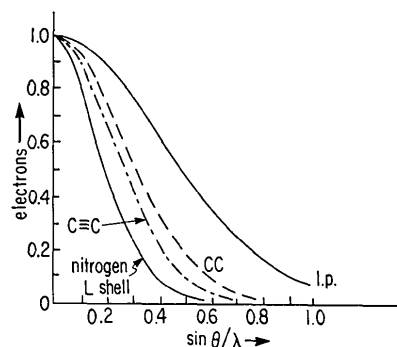
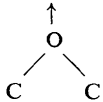
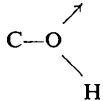
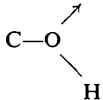
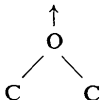
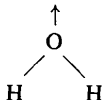
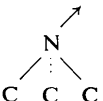


Fig. 8. Scattering factors for the difference density features in NCCN in the single Gaussian approximation.

Table 5. Sample of observed asphericity shifts

(1) Tetracyanoethylene oxide		0.013 (4) Å
(2) Tetracyanoethylene	$-\text{C} \rightarrow \text{N}$	0.008 <sub>s</sub> (1 <sub>s</sub> )
(3) Oxalic acid		0.008 (2)
(4) Sucrose	 and 	0.008 (2) 0.007 (2)
(5) Ammonium oxalate H <sub>2</sub> O		0.013 (3)
(6) Hexamethylene-tetramine		0.018 (6)
(7) Cyanuric acid	$\text{C}=\text{O} \rightarrow$	0.005 (1)

sophisticated calculations. In addition to a further reduction of experimental errors, allowance for thermal modification of the density and measurement of the absolute scale of the intensity data are required for the extraction of really quantitative information. Even at present, measurements on large molecules can provide chemical information not accessible by approximate calculations. The results on benzenechromium tricarbonyl indicate that densities in molecules with third row atoms can be studied successfully. Further studies may also elucidate the effect of the crystal matrix on molecular electron densities.

Support of this work by the National Science Foundation is gratefully acknowledged.

## References

- BECKER, P., COPPENS, P. & ROSS, F. K. (1973). *J. Amer. Chem. Soc.* **95**, 7604.
- BRILL, H., DIETRICH, H. & DIERKS, H. (1971). *Acta Cryst.* **B27**, 2003–2018.
- COPPENS, P. (1967). *Science*, **158**, 1577.
- COPPENS, P. (1971). *Acta Cryst.* **B27**, 1931–1938.
- COPPENS, P. (1972). *Israel J. Chem.* pp. 85–91.
- COPPENS, P. & COULSON, C. A. (1967). *Acta Cryst.* **23**, 718–720.
- COPPENS, P. & HAMILTON, W. C. (1968). *Acta Cryst.* **B24**, 925–929.
- COPPENS, P., SABINE, T. M., DELAPLANE, R. G. & IBERS, J. A. (1969). *Acta Cryst.* **B25**, 2451–2458.
- COPPENS, P. & VOS, A. (1971). *Acta Cryst.* **B27**, 146–158.
- COULSON, C. A. & MOFFITT, W. E. (1949). *Phil. Mag.* **40**, 1–10.
- CRUICKSHANK, D. W. J. (1949). *Acta Cryst.* **2**, 65–82.
- CRUICKSHANK, D. W. J. & ROLLETT, J. S. (1953). *Acta Cryst.* **6**, 705–707.
- DUCKWORTH, J. A. K., WILLIS, B. T. M. & PAWLEY, G. S. (1970). *Acta Cryst.* **A26**, 263–271.
- HANSON, J. C., SIEKER, L. C. & JENSEN, L. H. (1973). *Acta Cryst.* **B29**, 797–808.
- HIGGS, P. W. (1953). *Acta Cryst.* **6**, 232–241.
- HIRSHFELD, F. L. (1971). *Acta Cryst.* **B27**, 769–781.
- JONES, D. S., PAUTLER, D. & COPPENS, P. (1972). *Acta Cryst.* **A28**, 635–645.
- MATTHEWS, D. A. & STUCKY, G. D. (1971). *J. Amer. Chem. Soc.* **93**, 5954–5959.
- REES, B. & COPPENS, P. (1973). *Acta Cryst.* **B29**, 2516–2528.
- STEWART, R. F. (1968). *Acta Cryst.* **A24**, 497–505.
- TAYLOR, J. C. & SABINE, T. M. (1972). *Acta Cryst.* **B28**, 3340–3351.
- WILLIS, B. T. M. (1969). *Acta Cryst.* **A25**, 277–300.

*Acta Cryst.* (1974). **B30**, 261

## The Reliability of Crystallographic Structural Information\*

BY S. C. ABRAHAMS

*Bell Laboratories, Murray Hill, New Jersey 07974, U.S.A.*

(Received by the Hamilton Symposium Committee 15 June 1973)

A review is presented, drawn largely from the work of Walter Hamilton, of the optimal design of a crystallographic experiment, of structure-factor measurement and the estimation of associated standard deviations, of pitfalls connected with the large scale computations required for structural refinement, of methods for choosing the best structural model derivable from the experiment, of means for assessing the quality of the information finally extracted, and of tests for recognizing aberrant data after refinement is complete.

### 1. Introduction

The field that the present paper seeks to review as part of the Hamilton Symposium is one that long held a central place in Walter Hamilton's crystallographic interests, and to which he made many major contributions. The field is concerned with the derivation of objective methods for assessing the quality of experimental integrated intensity measurements, and with the improvement both of the measurements and their associated correction factors: with the error in the theoretical models used in crystal structure refinement and with the associated computing methods; with choosing among alternative models derived from a crystallographic experiment; and with assessing the significance of the final parameters determined in the refinement.

It is hoped this review will help underscore the coherence and importance of this aspect of Walter Hamilton's work, and at the same time highlight the broad conceptual framework in which he habitually thought.

### 2. Optimum experimental design

#### 2(a). Integrated intensity measurement

The best strategy for achieving the maximum precision in a crystallographic experiment of given duration has been frequently discussed since Parrish (1956) and Mack & Spielberg (1958) showed, for the case of X-ray powder diffractometry, that the optimum division of time between background determination and peak scanning is proportional to the ratio of the square roots of their respective counting rates. This result is based on the assumption of a Gaussian distribution of diffracted X-ray quanta with variance given by the mean. Extension to the single-crystal diffractometry case was made in a group of three papers (Hamilton, 1967; Shoemaker, 1968; Shoemaker & Hamilton,

\*Editorial note: – This paper was presented at a memorial symposium in honour of Walter C. Hamilton, a former Co-editor of *Acta Crystallographica*, held on 15 June 1973 at Brookhaven National Laboratory, and sponsored jointly by the American Crystallographic Association and the Brookhaven National Laboratory.